particles, $\bar{x} \lesssim S_{\bar{x}}$. Therefore, from measured y displacements, an equivalent particle size was calculated using Einstein's equation and from the size, a uniform temperature fall velocity for the particle was established. The difference between the total fall velocity and the calculated uniform temperature fall velocity is the thermal velocity from which the temperature gradient was estimated. Because the thermal velocity is the difference of two numbers of the same magnitude and because the vertical particle velocity error ranges from 4 to 40% and the uniform temperature fall velocity error (~twice the particle size error) from 20 to 40%, a sizable uncertainty in the gradient results. These additional data are shown in Fig. 1. The cross-hatched bands are only used to indicate the general data trend for the smoke particles and the oil drops. Particles 5, 8, and 13 might have agreed more with the trend if the gradient had been measured at the particle position instead of being extrapolated as was previously mentioned.

Several conclusions drawn from the work are listed in the order of decreasing experimental certainty.

(1) Anisotropy of random particle displacements ($\Delta x^2/\Delta y^2 \neq 1$) is believed to exist and to have been measured.

(2) The anisotropy is a function of the temperature gradient in the gas.

(3) A vertical (y) temperature gradient more significantly affects the Brownian fluctuations in the x than in the y direction.

(4) The change in anisotropy with temperature gradient is approximately the same for oil and smoke particles.

The region in which to begin an accurate analysis of the effect on Brownian motion of particle material, particle shape, particle size, temperature gradient and mean temperature, particle velocity, and gas composition would be in a constant-temperature cell.

Some of the measurements described here were made at Lehigh University. The author acknowledges the helpful discussions with R. J. Emrich, C. W. Curtis, and N. Oshima and the thermal conductivity measurements by R. U. Acton at Sandia Corporation.

The author notes his appreciation of partial support while at Lehigh by the National Science Foundation and subsequent support by the Atomic Energy Commission at Sandia Corporation.

[1] R. M. Elrick, Phys. Fluids 9, 10 (1966).
[2] W. M. Elsasser (private communication).
[3] H. Fletcher, Phys. Rev. 33, 81 (1911).
[4] R. M. Elrick and R. J. Emrich, Phys. Fluids 9, 28 (1966).
[5] P. Rosenblatt and V. K. LaMer, Phys. Rev. 70, 385 (1946).
[6] C. F. Schadt and R. D. Cadle, J. Colloid. Sci. 12, 356 (1957).
[7] M. R. Samuels and S. W. Churchill, A.I. Ch. E. J. 13, 77 (1967).

Equations for Gas Mixtures. II

EDWARD GOLDMAN
Department of Mechanical and Aerospace Sciences, University of Rochester Rochester, New York
AND
LAWRENCE SIROVICH
Division of Applied Mathematics and the Center for Fluid Dynamics, Brown University Providence, Rhode Island
(Received 14 March 1968)

An extension of a previous paper on the equations governing gas mixtures is presented. Revision of the relaxation time of component velocities leads to a new diffusion equation. Various dimensionless parameters of a binary gas are plotted.

In a previous paper[1] we examined the Chapman–Enskog procedure for gas mixtures. There, it was discovered that in a variety of situations it is necessary to include the effect of individual component temperatures and, therefore, to consider somewhat generalized equations. The key parameter C in such a discussion is related to the Schmidt number Sc through

$$C = \frac{2\rho \, \mathrm{Sc}}{n(m_\alpha + m_\beta)},$$

where we have used the same notation as in I. In Fig. 1 we have plotted the modified Schmidt number C as well as Sc for an argon–helium and a xenon–helium mixture, respectively. As in I, the transport data needed for these curves are partly based on experiment and partly on theoretical formulas. It should be noted that C displays far less dependence on m_α/m_β and n_α/n than does Sc. For this reason it might be more useful to employ C instead of Sc in a number of situations.

From I we recall that the derivation of fluidlike

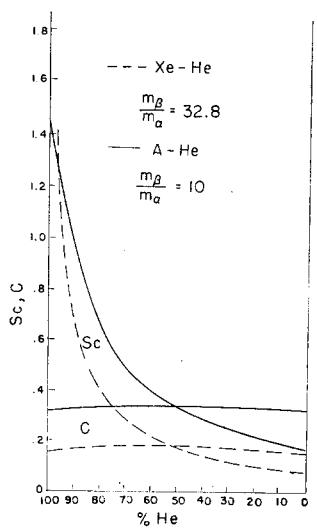

FIG. 1. C and Sc for Ar–He and Xe–He mixtures at normal temperature and pressure.

Downloaded 16 Jun 2008 to 146.203.28.10. Redistribution subject to AIP license or copyright; see http://pof.aip.org/pof/copyright.jsp

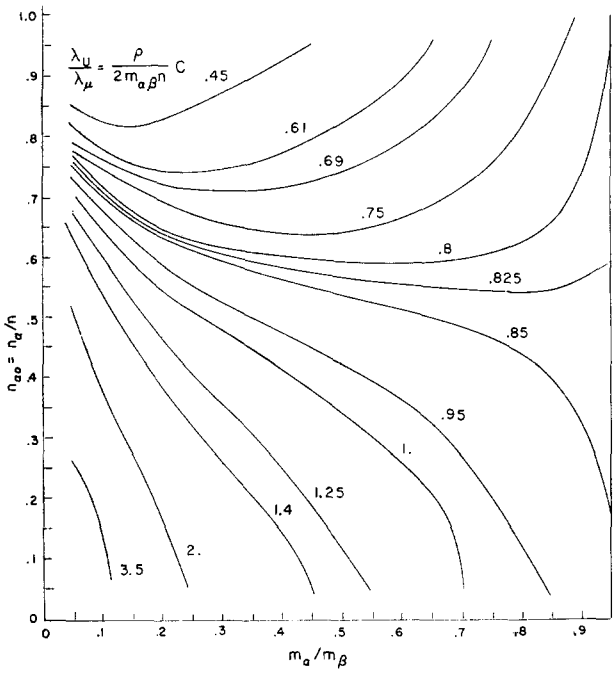

FIG. 2. $\lambda_U/\lambda_\mu = \rho C/(2m_{\alpha\beta}n)$—rigid-sphere molecules.

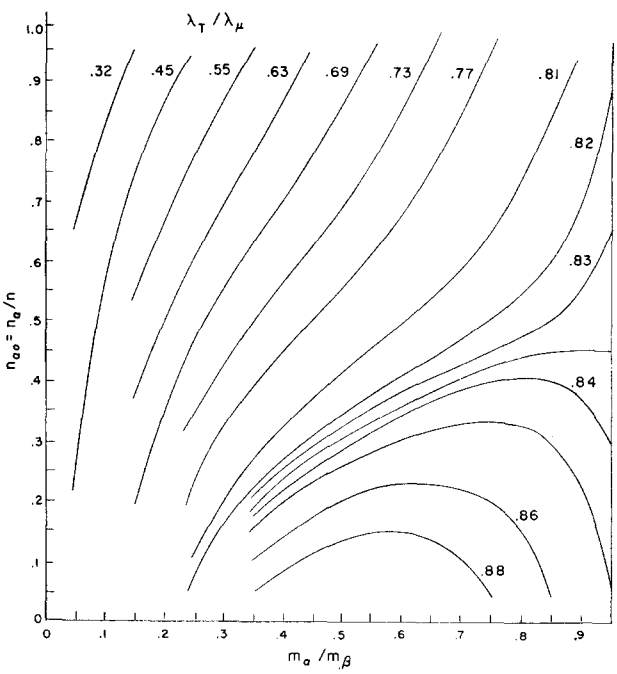

FIG. 3. $\lambda_T/\lambda_\mu = C$—rigid-sphere molecules.

mixture equations from the Boltzmann equations for mixtures follows from an analysis of three microscopic scales. These are: λ_U^{-1}, the time scale on which component velocity differences vanishes; λ_T^{-1}, the time scale on which component temperature differences vanish; λ_s^{-1}, the time scale on which the component distribution functions become locally Maxwellian.

Owing to an incorrect estimate in considering λ_U/λ_s, we erroneously stated in I that this ratio is always greater than unity. In fact regarding Eq. (52) of Ref. 1 we see that

$$\lim (\lambda_T/\lambda_U) = 2,$$

$$m_\alpha/m_\beta \to 0,$$

$$\rho_\alpha/\rho \to 1.$$

(This is the maximum of this ratio.) Then, in view of the inequality below Eq. (52) of Ref. 1 we see that λ_s can exceed λ_U. Rather than λ_s it is more convenient to use the viscosity-based frequency

$$\lambda_\mu = p/\mu.$$

(From I, Sec. IV-c, it can be seen that $\lambda_\mu \approx \lambda_s$.) Then, from Eqs. (52) and (60) of Ref. 1

$$\frac{\lambda_U}{\lambda_\mu} = \frac{\rho}{2m_{\alpha\beta}n} C = \frac{m_T^2}{m_\alpha m_\beta} \mathrm{Sc},$$

where

$$m_T = \rho/n.$$

In Figs. 2 and 3 we have plotted λ_U/λ_μ and $\lambda_T/\lambda_\mu = C$, respectively for rigid sphere molecules. (The last is a replot of I; Fig. 2 in a more convenient form.)

In view of the fact that λ_U/λ_μ can be small (the upper left-hand portion of Fig. 2) the full two-fluid equations (I; Sec. III) have a wider application than was suggested in I. This is also of importance in connection with the generalized Chapman–Enskog procedure (I; Sec. IV). In fact, when λ_U/λ_μ is small the curly-bracket term of Eq. (46) of Ref. 1 can no longer be regarded as ignorable. Since the generalized Chapman–Enskog procedure (I; Sec. IV) considers situations in which $(\mathbf{U}_\alpha - \mathbf{U}_\beta)$ is small (i.e., when properly normalized as noted in Ref. 7 of I), the curly bracket can be simplified. To accomplish this we note that

$$\frac{\mathbf{U}_\alpha + \mathbf{U}_\beta}{2} = \mathbf{U} + \frac{(\rho_\beta - \rho_\alpha)(\mathbf{U}_\alpha - \mathbf{U}_\beta)}{2\rho}. \tag{1}$$

Substituting this into Eq. (46) of I and proceeding with the perturbation procedure of I: Sec. IV, we obtain instead of the diffusion equation [Eq. (48) of I],

$$\frac{\partial}{\partial t}(\mathbf{U}_\alpha - \mathbf{U}_\beta) + \frac{\partial}{\partial x_i}[U_i(\mathbf{U}_\alpha - \mathbf{U}_\beta)] + \lambda_U(\mathbf{U}_\alpha - \mathbf{U}_\beta)$$
$$= -\frac{\rho p}{\rho_\alpha \rho_\beta}\left[\nabla\left(\frac{n_\alpha}{n}\right) + \frac{1}{p}\nabla\left(\frac{n_\alpha n_\beta k(T_\alpha - T_\beta)}{n}\right) - \frac{n_\alpha n_\beta}{n^2 T}\eta\nabla T + \frac{m_\alpha n_\beta(m_\beta - m_\alpha)}{n\rho}\nabla \ln p\right]. \tag{2}$$

In the above we have included the thermodiffusion effect which was ignored (I). Expressions for η may

Downloaded 16 Jun 2008 to 146.203.28.10. Redistribution subject to AIP license or copyright; see http://pof.aip.org/pof/copyright.jsp

be found in the literature.[2] The heat flow equation [Eq. (55) of I] must then also be augmented by the diffusion-thermo effect and we have instead

$$\mathbf{Q} = -\kappa\nabla T + \frac{5}{2}kT\frac{n_\alpha n_\beta(m_\beta - m_\alpha)}{\rho}(\mathbf{U}_\alpha - \mathbf{U}_\beta) + \frac{n_\alpha n_\beta}{n^2}p\eta(\mathbf{U}_\beta - \mathbf{U}_\alpha). \quad (3)$$

Therefore the equations of the generalized Chapman–Enskog procedure now are: Eqs. (13), (27), (28), (29), (53), (54) of I and (2) and (3) from the above. When $\lambda_U/\lambda_\mu \geq O(1)$ we return to the two temperature equations of I. To see this we merely note that the differential operator on the left-hand side of (2) becomes negligible compared to

$$\lambda_U(\mathbf{U}_\alpha - \mathbf{U}_\beta)$$

and this equation reduces to the diffusion equation [Eq. (48) of I]. Finally the classical Chapman–Enskog mixture equations are obtained as before under the condition of Eq. (56) of I. In this last situation two temperature effects are higher order. The expressions for component temperatures can then be computed from the flow field through the "temperature diffusion" equation (58) of I.

The results communicated in this paper were obtained in the course of research sponsored by the Office of Naval Research under Contract Nonr 562(39).

[1] E. Goldman and L. Sirovich, Phys. Fluids **10**, 1928 (1967). This will be referred to as I.
[2] For example, Refs. 2 and 8 of I.

Transport Cross Sections for Screened and Cutoff Coulomb Potentials

KURT SUCHY
Institute for Theoretical Physics, University of Marburg
Marburg, Germany
(Received 9 July 1968; final manuscript received 10 October 1968)

The analytic expressions for the transport cross sections of a cutoff Coulomb potential agree with the numerical results of an exponentially screened potential if the cutoff radius is suitably related to the screening Debye–Hückel length and the Landau length.

For transport processes in weakly ionized plasmas it is desirable to describe the interactions of charges (approximately) by means of binary collisions. This description facilitates the comparison of these effects with those of charge–neutral interactions. For the latter the binary collision description is justified because of the short-range character of the interaction potentials.

Since the integrals for the collision cross sections diverge for a Coulomb potential (because of its long-range character), it has to be modified to ensure convergence. From a physical point of view the most satisfying modification is an exponential screening in accordance with the Debye–Hückel theory[1] of charge clouds around a test particle. Unfortunately, the velocity dependence of the corresponding collision cross sections cannot be completely expressed in terms of analytic functions. Consequently, the temperature dependence of the (velocity-averaged) transport cross sections has to be computed numerically for a wide range of temperatures.[2]

This disadvantage can be avoided with a cutoff Coulomb potential. Of course, this crude modification is physically less satisfying than the exponential screening. But the velocity dependence of the collision cross sections can be expressed completely in terms of logarithms and derivatives of Legendre polynomials; the temperature dependence of the transport cross sections is expressed by exponential functions and exponential integrals.[3]

For the temperature dependence of the transport cross sections the advantages of both models can be combined by an appropriate choice of the cutoff radius σ in the cutoff Coulomb potential

$$U(r) = \frac{q_i q_j}{4\pi\epsilon_0}\begin{cases} r^{-1} & \text{for} \quad r \leq \sigma \\ \sigma^{-1} & \text{for} \quad r \geq \sigma. \end{cases} \quad (1)$$

The collision cross sections $Q^{(l)}(g)$ for a binary collision between charges q_i and q_j are given[4] by the integration of $1 - P_l(\cos\chi)$ over the differential cross section $dQ(\chi, g)$. (g is the relative speed; the Legendre polynomials P_l depend on the deflection angle χ.) The transport cross sections $q^{(l|m)}$ times the most probable relative speed are velocity averages of $gQ^{(l)}(g)$ with g^{2m} times the Maxwellian velocity distributions of both colliding partners as weight functions.[5] They are directly related[5] to the $\Omega^{(l,s)}$ of Hirschfelder–Curtiss–Bird.[6]

With the Landau length

$$\hat{a} \equiv \frac{q_i q_j}{4\pi\epsilon_0}\left(\frac{1}{m_i} + \frac{1}{m_j}\right)\left(\frac{2kT_i}{m_i} + \frac{2kT_j}{m_j}\right)^{-1} \gtrless 0 \quad \text{for} \quad \begin{matrix}\text{repulsion} \\ \text{attraction,}\end{matrix}$$

the (dimensionless) quantities $q^{(l|m)}/\pi(2\hat{a})^2$ depend only on the ratio of $\hat{a}$ and a characteristic length of the interaction potential. This ratio is $\hat{a}/\sigma$ for the cutoff Coulomb potential (1) and the plasma

Downloaded 16 Jun 2008 to 146.203.28.10. Redistribution subject to AIP license or copyright; see http://pof.aip.org/pof/copyright.jsp